PERGAMON

International Journal of Solids and Structures 38 (2001) 8617–8640

INTERNATIONAL JOURNAL OF SOLIDS and STRUCTURES

www.elsevier.com/locate/ijsolstr

Elastic/plastic buckling of thick plates

C.M. Wang [a,*], Y. Xiang [b], J. Chakrabarty [c]

[a] *Department of Civil Engineering, National University of Singapore, Kent Ridge, Singapore 119260, Singapore*
[b] *School of Engineering and Industrial Design, University of Western Sydney, Penrith South DC, NSW 1797, Australia*
[c] *10 Mayfair Road, Apartment #101, Calcutta 700 019, India*

Received 22 December 2000; in revised form 14 May 2001

Abstract

This paper is concerned with the elastic/plastic buckling of thick plates of rectangular and circular shapes. For thick plates, the significant effect of transverse shear deformation on the critical buckling load may be accounted for by adopting the Mindlin plate theory. To capture the elastic/plastic behaviour, two competing theories of plasticity are considered; viz. the incremental theory (IT) of plasticity (with the Prandtl–Reuss constitutive relations) and the deformation theory (DT) of plasticity (with the Hencky constitutive relation). Analytical elastic/plastic stability criteria are derived for (a) uniaxially and equibiaxially loaded rectangular plates with two opposite edges simply supported while the other two edges may take on any combination of free, simply supported or clamped boundary condition and (b) uniformly inplane loaded circular plates with either simply supported edge or clamped edge. Extensive buckling stress factors are tabulated for these plates with material properties defined by the Ramberg–Osgood relation. Comparing the results obtained from the DT and the IT, it can be seen that not only the DT in general gives consistently lower values of buckling stress factor but the divergence of the results from the two theories increases with increasing plate thicknesses, E/σ_0 values and c values of the Ramberg–Osgood relation. The buckling results from the two theories and their marked difference from each other for thick plates may be exploited in the design of experimental tests to ascertain which one of the two theories provides good estimates of the buckling loads for thick plates.

Keywords: Elastic/plastic buckling; Thick plates; Incremental theory of plasticity; Deformation theory of plasticity; Rectangular plates; Circular plates

1. Introduction

Elastic bifurcation and postbuckling behaviour of thin plates have been extensively studied and well documented in standard texts (e.g. Timoshenko and Gere, 1961; Bazant and Cedolin, 1991). When the plate thickness to length ratio is greater than 1/20, it is necessary to use thick plate theories such as the Mindlin (1951) plate theory to calculate the buckling load. Otherwise the buckling load will be overestimated because in thick plates the effect of transverse shear deformation is significant. Elastic buckling of Mindlin

* Corresponding author. Tel.: +65-874-2157; fax: +65-779-1635.
E-mail addresses: cvewcm@nus.edu.sg (C.M. Wang), y.xiang@uws.edu.au (Y. Xiang).

0020-7683/01/$ - see front matter
PII: S0020-7683(01)00144-5

plates has been investigated by many researchers (for example, Herrmann and Armenakas, 1960; Brunelle, 1971; Kanaka Raju and Venkateswara Rao, 1983; Chen and Doong, 1984; Dumir, 1985; Hong et al., 1993; Wang et al., 1993; Wang, 1995; Wang et al., 1996).

The elastic buckling load is useful as an upper bound solution and a basic reference parameter in design codes. For a more advanced bifurcation buckling analysis, various elastic/plastic theories have been proposed, which may be categorized under the incremental (or flow) theory (IT) of plasticity (e.g. Handelman and Prager, 1948; Pearson, 1950), the deformation theory (DT) of plasticity (e.g. Kaufmann, 1936; Illyushin, 1947; Stowell, 1948; Bijlaard, 1949; El-Ghazaly and Sherbourne, 1986), or the slip theory (e.g. Bartdorf, 1949; Inoue and Kato, 1993). The success of these is varied. For example, the DT gives a better prediction of buckling loads for long simply supported plates while the IT gives better results for cylinders under compression and torsion. Accordingly, some researchers (e.g. Shrivastava, 1979; Ore and Durban, 1989; Tugcu, 1991; Durban and Zuckerman, 1999) presented the elastic/plastic buckling loads of plates based on both the deformation-type theory and the incremental-type theory. There are, however, other simplified theories such as the one proposed by Bleich (1952). Bleich assumed a two-moduli plate where the modulus in the direction of stress that is likely to exceed the proportional limit be taken as the tangent modulus T while in the direction where there is little stress, the elastic modulus E be taken. Furthermore, the factor for the twisting moment curvature relation is arbitrarily chosen as $(T/E)^{1/2}$. Bleich's simplified theory seems to give results in close agreement with large-scale test results obtained by Kollbrunner (1946).

Apart from the paper by Shrivastava (1979), the aforementioned studies on elastic/plastic buckling analysis of plates adopted the classical thin plate theory. When dealing with thick plates where buckling occurs in the plastic range, a shear deformable plate theory has to be employed so as to admit the significant effect of transverse shear deformation. Complementing the work of Shrivastava (1979), the present study adopts the Mindlin plate theory for the elastic/plastic buckling of rectangular thick plates under equibiaxial and uniaxial loading, and of circular thick plates under a uniform radial load. Two plasticity theories are considered; i.e. the IT of plasticity with the Prandtl–Reuss constitutive equations and the DT of plasticity with the Hencky stress–strain relation. An important difference between these two theories is that the strain in the former theory depends on the manner in which the state of stress is built up, whereas in the latter theory the strain that corresponds to a certain state of stress is entirely independent of the manner in which this state of stress has been reached. Analytical elastic/plastic stability criteria are derived for rectangular and circular thick plates for both theories. Extensive buckling stress factors, from both theories of plasticity, are tabulated for square and circular plates whose materials exhibit strain hardening characterized by the Ramberg–Osgood stress–strain relation. These basic results should be useful to engineers who are designing plate structures subject to inplane loadings and to researchers planning to perform buckling experiments on thick plates so as to ascertain which of the two aforementioned theories gives a better estimate of the buckling loads of thick plates.

2. Buckling of rectangular plates

2.1. Basic equations

Consider a flat, rectangular plate whose sides are of lengths a and b and of uniform thickness h as shown in Fig. 1. The plate is acted upon by uniform compressive stresses of magnitudes σ_1 and σ_2 in the x- and y-direction, respectively. According to the Mindlin plate theory (Mindlin, 1951), the admissible velocity field may be written as

$$v_x = z\phi_x; \qquad v_y = z\phi_y; \qquad v_z = w \tag{1}$$

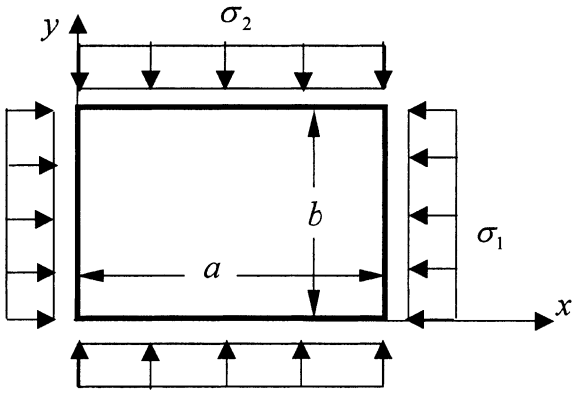

Fig. 1. Elastic/plastic buckling of rectangular plates.

where ϕ_x and ϕ_y are the rotation rates about the y- and x-axes, respectively, and w is the transverse velocity. The strain rates corresponding to Eq. (1) are given by

$$\begin{aligned} &\dot{\varepsilon}_{xx} = z\frac{\partial \phi_x}{\partial x}; \qquad \dot{\varepsilon}_{yy} = z\frac{\partial \phi_y}{\partial y} \\ &\dot{\gamma}_{xy} = z\left(\frac{\partial \phi_x}{\partial y} + \frac{\partial \phi_y}{\partial x}\right); \qquad \dot{\gamma}_{xz} = \phi_x + \frac{\partial w}{\partial x}; \qquad \dot{\gamma}_{yz} = \phi_y + \frac{\partial w}{\partial y} \end{aligned} \tag{2}$$

The constitutive relations of the Prandtl–Reuss type as well as the Hencky type for a linearized elastic/plastic solid that behaves identically under loading and unloading, are given by (Chakrabarty, 2000)

$$\begin{aligned} &\dot{\sigma}_{xx} = E(\alpha\dot{\varepsilon}_{xx} + \beta\dot{\varepsilon}_{yy}); \qquad \dot{\sigma}_{yy} = E(\beta\dot{\varepsilon}_{xx} + \gamma\dot{\varepsilon}_{yy}) \\ &\dot{\tau}_{xy} = G\dot{\gamma}_{xy}; \qquad \dot{\tau}_{xz} = \kappa^2 G\dot{\gamma}_{xz}; \qquad \dot{\tau}_{yz} = \kappa^2 G\dot{\gamma}_{yz} \end{aligned} \tag{3}$$

where E is the elastic modulus, G the effective shear modulus, and κ^2 the Mindlin shear correction factor to compensate for the error in assuming a constant shear strain (hence a constant shear stress) through the plate thickness.

The expressions of α, β, γ, ρ and the shear modulus are given by (see Appendices A and B for their derivations):

In the case of the incremental theory:

$$\begin{aligned} \alpha &= \frac{1}{\rho}\left[4 - 3\left(1 - \frac{T}{E}\right)\frac{\sigma_1^2}{\bar{\sigma}^2}\right] \\ \beta &= \frac{1}{\rho}\left[2 - 2(1-2\nu)\frac{T}{E} - 3\left(1 - \frac{T}{E}\right)\frac{\sigma_1\sigma_2}{\bar{\sigma}^2}\right] \\ \gamma &= \frac{1}{\rho}\left[4 - 3\left(1 - \frac{T}{E}\right)\frac{\sigma_2^2}{\bar{\sigma}^2}\right] \\ \rho &= (5-4\nu) + (1-2\nu)^2\frac{T}{E} - 3(1-2\nu)\left(1 - \frac{T}{E}\right)\frac{\sigma_1\sigma_2}{\bar{\sigma}^2} \\ \frac{E}{G} &= 2(1+\nu) \end{aligned} \tag{4}$$

In the case of the deformation theory:

$$\alpha = \frac{1}{\rho}\left[4 - 3\left(1 - \frac{T}{S}\right)\frac{\sigma_1^2}{\bar{\sigma}^2}\right]$$
$$\beta = \frac{1}{\rho}\left[2 - 2(1-2\nu)\frac{T}{E} - 3\left(1 - \frac{T}{S}\right)\frac{\sigma_1\sigma_2}{\bar{\sigma}^2}\right]$$
$$\gamma = \frac{1}{\rho}\left[4 - 3\left(1 - \frac{T}{S}\right)\frac{\sigma_2^2}{\bar{\sigma}^2}\right] \tag{5}$$
$$\rho = 3\frac{E}{S} + (1-2\nu)\left[2 - (1-2\nu)\frac{T}{E} - 3\left(1 - \frac{T}{S}\right)\frac{\sigma_1\sigma_2}{\bar{\sigma}^2}\right]$$
$$\frac{E}{G} = 2 + 2\nu + 3\left(\frac{E}{S} - 1\right)$$

wherein the ratios of the elastic modulus E to the tangent modulus T, and the secant modulus S at the onset of buckling are expressed by the Ramberg–Osgood elastoplastic characteristic in the forms of

$$\frac{E}{T} = 1 + ck\left(\frac{\bar{\sigma}}{\sigma_0}\right)^{c-1}; \quad c > 1 \tag{6}$$

$$\frac{E}{S} = 1 + k\left(\frac{\bar{\sigma}}{\sigma_0}\right)^{c-1}; \quad c > 1 \tag{7}$$

where σ_0 is a nominal yield stress, c is a dimensionless constant that describes the shape of the stress–strain relationship with $c = \infty$ for elastic–perfectly plastic response, k the horizontal distance between the knee of $c = \infty$ curve and the intersection of the c curve with the $\sigma/\sigma_0 = 1$ line as shown in Fig. 2. The equivalent stress $\bar{\sigma}$ is defined on the basis of von Mises yield criterion given by

$$\bar{\sigma}^2 = \sigma_1^2 - \sigma_1\sigma_2 + \sigma_2^2 \tag{8}$$

Note that by setting the secant modulus S in Eq. (5) to be equal to the elastic modulus (i.e. $S = E$), the expressions of α, β, γ, ρ of the Hencky DT reduce to those corresponding to the IT with Prandtl–Reuss equations.

To obtain the condition for bifurcation of the plate in the elastic/plastic range, it is assumed that Shanley's concept of continued loading during buckling is accepted and therefore, no unloading takes place. Consider the uniqueness criterion in the form (Chakrabarty, 2000)

$$\int\left\{(\dot{\sigma}_{xx}\dot{\varepsilon}_{xx} + \dot{\sigma}_{yy}\dot{\varepsilon}_{yy} + \dot{\tau}_{xy}\dot{\gamma}_{xy} + \dot{\tau}_{xz}\dot{\gamma}_{xz} + \dot{\tau}_{yz}\dot{\gamma}_{yz}) - \sigma_1\left(\frac{\partial w}{\partial x}\right)^2 - \sigma_2\left(\frac{\partial w}{\partial y}\right)^2\right\}\mathrm{d}V > 0 \tag{9}$$

Using Eqs. (3) and (4) and integrating through the thickness of the plate, the condition for uniqueness is reduced to

$$\int\int\left\{\frac{\alpha E h^3}{12}\left(\frac{\partial\phi_x}{\partial x}\right)^2 + \frac{\gamma E h^3}{12}\left(\frac{\partial\phi_y}{\partial y}\right)^2 + \frac{\beta E h^3}{6}\left(\frac{\partial\phi_x}{\partial x}\right)\left(\frac{\partial\phi_y}{\partial y}\right) + \frac{G h^3}{12}\left(\frac{\partial\phi_x}{\partial x} + \frac{\partial\phi_y}{\partial y}\right)^2 + \kappa^2 G h\left[\left(\phi_x + \frac{\partial w}{\partial x}\right)^2 + \left(\phi_y + \frac{\partial w}{\partial x}\right)^2\right] - \sigma_1 h\left(\frac{\partial w}{\partial x}\right)^2 - \sigma_2 h\left(\frac{\partial w}{\partial y}\right)^2\right\}\mathrm{d}x\,\mathrm{d}y > 0 \tag{10}$$

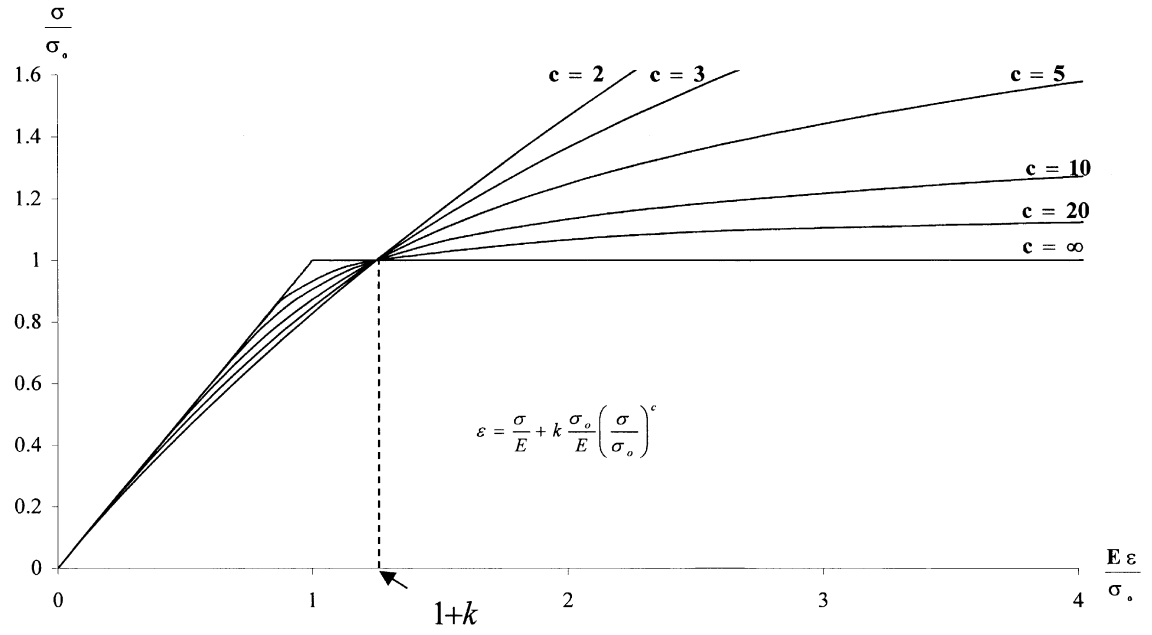

Fig. 2. Ramberg–Osgood stress–strain relation.

The Euler–Lagrange differential equations associated with the minimization with respect to arbitrary variations of w, ϕ_x, ϕ_y are easily shown to be

$$\kappa^2 Gh\left(\frac{\partial\phi_x}{\partial x}+\frac{\partial\phi_y}{\partial y}+\nabla^2 w\right)=\sigma_1 h\frac{\partial^2 w}{\partial x^2}+\sigma_2 h\frac{\partial^2 w}{\partial y^2} \tag{11a}$$

$$\frac{\partial}{\partial x}\left(\frac{\alpha Eh^3}{12}\frac{\partial\phi_x}{\partial x}+\frac{\beta Eh^3}{12}\frac{\partial\phi_y}{\partial y}\right)+\frac{\partial}{\partial y}\left[\frac{Gh^3}{12}\left(\frac{\partial\phi_x}{\partial y}+\frac{\partial\phi_y}{\partial x}\right)\right]-\kappa^2 Gh\left(\phi_x+\frac{\partial w}{\partial x}\right)=0 \tag{11b}$$

$$\frac{\partial}{\partial y}\left(\frac{\gamma Eh^3}{12}\frac{\partial\phi_y}{\partial y}+\frac{\beta Eh^3}{12}\frac{\partial\phi_x}{\partial x}\right)+\frac{\partial}{\partial x}\left[\frac{Gh^3}{12}\left(\frac{\partial\phi_x}{\partial y}+\frac{\partial\phi_y}{\partial x}\right)\right]-\kappa^2 Gh\left(\phi_y+\frac{\partial w}{\partial y}\right)=0 \tag{11c}$$

If the tangent modulus and the secant modulus at the point of bifurcation is the same as the elastic modulus, i.e. $T=S=E$, we have

$$\alpha=\gamma=\frac{1}{1-\nu^2} \tag{12a}$$

$$\beta=\frac{\nu}{1-\nu^2} \tag{12b}$$

and Eqs. (11a)–(11c) would then reduce to the well-known governing equation for elastic buckling of Mindlin plates (Brunelle, 1971; Wang, 1995).

2.2. Buckling solutions for simply supported rectangular plates

For a rectangular plate with simply supported edges as shown in Fig. 1, the boundary conditions are

$$w(0,y) = M_{xx}(0,y) = \phi_y(0,y) = 0 \tag{13a}$$

$$w(x,0) = M_{yy}(x,0) = \phi_x(x,0) = 0 \tag{13b}$$

$$w(a,y) = M_{xx}(a,y) = \phi_y(a,y) = 0 \tag{13c}$$

$$w(x,b) = M_{yy}(x,b) = \phi_x(x,b) = 0 \tag{13d}$$

where the bending moment rates are

$$M_{xx} = \frac{Eh^3}{12}\left(\alpha\frac{\partial\phi_x}{\partial x} + \beta\frac{\partial\phi_y}{\partial y}\right), \qquad M_{yy} = \frac{Eh^3}{12}\left(\beta\frac{\partial\phi_x}{\partial x} + \gamma\frac{\partial\phi_y}{\partial y}\right) \tag{14}$$

The rates of displacement and rotations that satisfy the foregoing boundary conditions are given by

$$w = C^w_{mn}\sin\left(\frac{m\pi x}{a}\right)\sin\left(\frac{n\pi y}{b}\right) \tag{15a}$$

$$\phi_x = C^{\phi_x}_{mn}\cos\left(\frac{m\pi x}{a}\right)\sin\left(\frac{n\pi y}{b}\right) \tag{15b}$$

$$\phi_y = C^{\phi_y}_{mn}\sin\left(\frac{m\pi x}{a}\right)\cos\left(\frac{n\pi y}{b}\right) \tag{15c}$$

where C^w_{mn}, $C^{\phi_x}_{mn}$, $C^{\phi_y}_{mn}$ are constants, $m, n = 1, 2, 3, \ldots$

The substitution of Eqs. (15a)–(15c) in Eqs. (11a)–(11c) results in the following three equations which may be expressed as:

$$\begin{bmatrix} A_{11} & A_{12} & A_{13} \\ & A_{22} & A_{23} \\ \text{sym} & & A_{33} \end{bmatrix} \begin{Bmatrix} C^w_{mn} \\ C^{\phi_x}_{mn} \\ C^{\phi_y}_{mn} \end{Bmatrix} = \begin{Bmatrix} 0 \\ 0 \\ 0 \end{Bmatrix} \tag{16}$$

where

$$A_{11} = \kappa^2 Gh\left(\frac{m^2\pi^2}{a^2} + \frac{n^2\pi^2}{b^2}\right) - \sigma_1 h\left(\frac{m^2\pi^2}{a^2}\right) - \sigma_2 h\left(\frac{n^2\pi^2}{b^2}\right) \tag{17a}$$

$$A_{12} = \kappa^2 Gh\left(\frac{m\pi}{a}\right) \tag{17b}$$

$$A_{13} = \kappa^2 Gh\left(\frac{n\pi}{b}\right) \tag{17c}$$

$$A_{22} = \frac{\alpha Eh^3}{12}\left(\frac{m^2\pi^2}{a^2}\right) + \frac{Gh^3}{12}\left(\frac{n^2\pi^2}{b^2}\right) + \kappa^2 Gh \tag{17d}$$

$$A_{23} = \left(\frac{\beta Eh^3}{12} + \frac{Gh^3}{12}\right)\left(\frac{mn\pi^2}{ab}\right) \tag{17e}$$

Table 1
Buckling stresses σ_c for a simply supported, square plate under uniaxial load

b/h	Buckling stresses σ_c in ksi		
	IT	DT	Bleich's theory[a]
22	70.844	60.080	56.125
23	65.166	58.836	55.139
24	60.713	57.397	54.109
25	57.363	55.730	52.988
26	54.598	53.806	51.712
27	51.938	51.569	50.185
28	49.112	48.962	48.269

[a] Note that Bleich's theory gives

$$\sigma_c = \frac{\pi^2 E\sqrt{T/E}}{12(1-\nu^2)}\left(\frac{h}{b}\right)^2\left[\frac{a/b}{n\sqrt[4]{T/E}}+\frac{T/E}{n\sqrt[4]{a/b}}\right]^2$$

where n is the number of half waves in which the plate buckles in the x-direction.

$$A_{33} = \frac{\gamma E h^3}{12}\left(\frac{n^2\pi^2}{b^2}\right)+\frac{Gh^3}{12}\left(\frac{m^2\pi^2}{a^2}\right)+\kappa^2 Gh \tag{17f}$$

The critical buckling stress can be determined by setting the determinant of the matrix $[A]$ in Eq. (16) to zero.

To assess the correctness of the foregoing formulation, we consider Shrivastava's square plate (i.e. $a = b$) constructed from 14S-T6 aluminium alloy where $E = 10{,}700$ ksi, $\nu = 0.32$, $\sigma_0 = 61.4$ ksi, the Ramberg–Osgood parameters $c = 20$ and $k = 0.3485$. The plate is subjected to a uniaxial load. The buckling stresses, obtained on the basis of the DT and the IT, are given in Table 1 for comparison purposes. These results are in very good agreement with Shrivastava's values that were plotted in Fig. 2 of his paper (Shrivastava, 1979). As expected, the use of the DT leads to a lower buckling stress value when compared to the corresponding value obtained using the IT, since the latter theory gives a stiffer response in the plastic range. Also, it can be seen from Table 1 that Bleich's buckling results, known to agree well with experimental test results, are closer to the results of the DT.

As presented in Figs. 3 and 4, critical buckling stress factors $\sigma_c hb^2/(\pi^2 D)$ are determined for simply supported, square plates with different thickness to width ratios h/b, and various values of c and E/σ_0. Note that $D = Eh^3/[12(1-\nu^2)]$ is the plate flexural rigidity. The Poisson ratio $\nu = 0.3$ and the shear correction factor $\kappa^2 = 5/6$ are used in all calculations. The plate is subjected to either a uniaxial inplane load or an equibiaxial inplane load. It can be observed that the buckling stress factors obtained by the DT are consistently lower than those obtained by the IT. Generally, the differences of results of these two theories increase with (a) increasing plate thickness (i.e. h/b values) as evident from Fig. 3a and b, and (b) increasing E/σ_0 values as can be seen from Fig. 4a and b. The Ramberg–Osgood constant c and the loading configuration (i.e. uniaxial load or equibiaxial loads) also affect the divergence of results from the two theories. It is interesting to note that both theories give somewhat similar results when the plate is thin, equibiaxially loaded and c value is large (say 20). Apart from the aforementioned situation, there is a marked difference in buckling stress factors from the two theories, which could be exploited when designing experimental tests on plates to establish which one of the theories gives better estimates of the buckling results for thick plates.

Fig. 5a presents the variations of the buckling stress factors, from the two theories, with respect to the aspect ratio a/b of uniaxially loaded, simply supported rectangular plates (of $h/b = 0.025$) for various values of c. It is worth noting that the kinks, where the number of half waves switches, are displaced as a result of transverse shear deformation as well as the inelastic characteristics. Fig. 5b shows the buckling

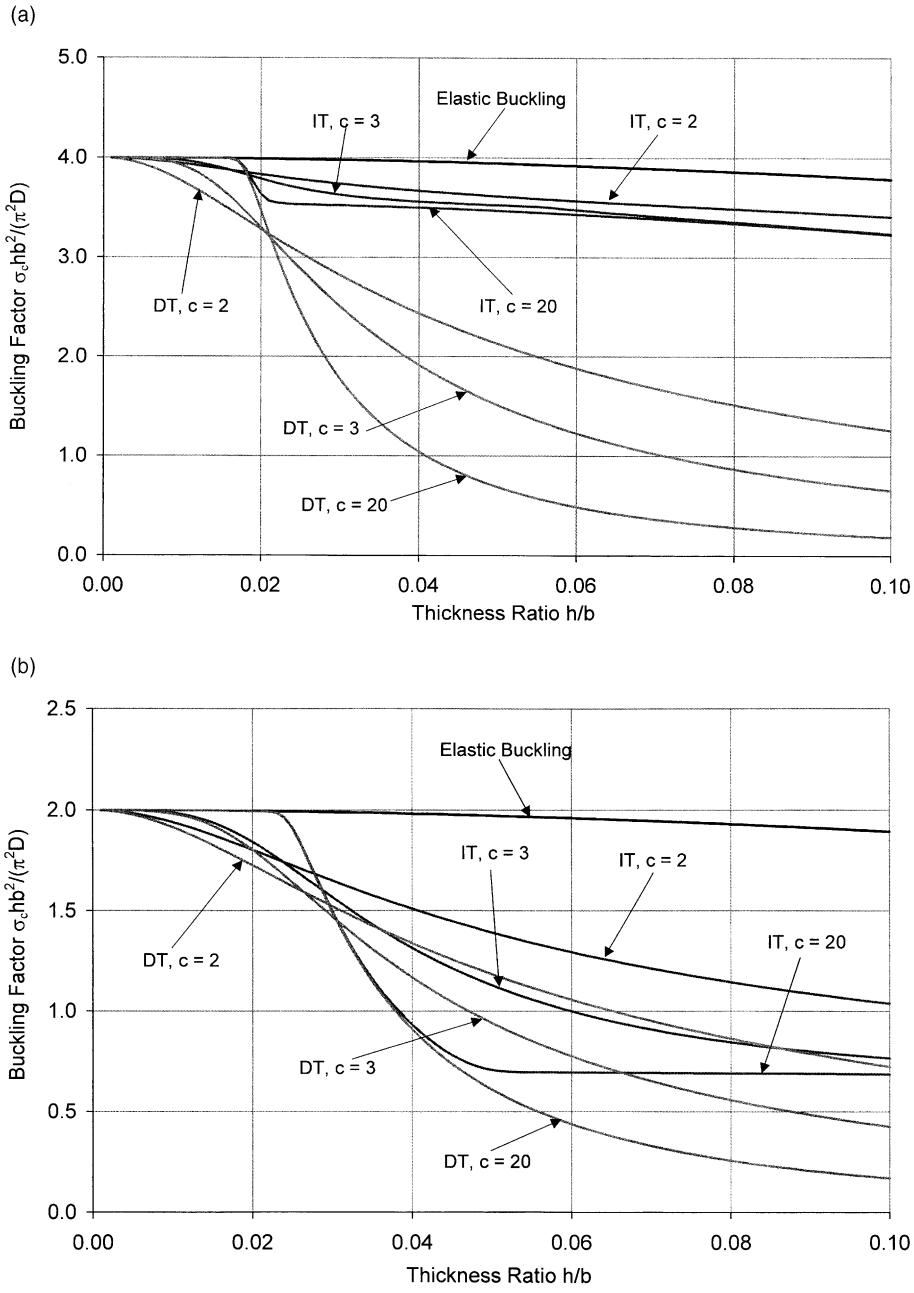

Fig. 3. Buckling stress factor $\sigma_c hb^2/(\pi^2 D)$ versus thickness ratio h/b for simply supported, square Mindlin plates subjected to (a) uniaxial load and (b) equibiaxial load ($E/\sigma_0 = 750,\ a/b = 1,\ \nu = 0.3,\ \kappa^2 = 5/6,\ k = 0.25$).

stress factor variations for equibiaxially loaded rectangular plates. In contrast to the uniaxial loaded plate case, there are no kinks in the variations of the buckling stress factors with respect to the aspect ratio, indicating that there is no mode switching.

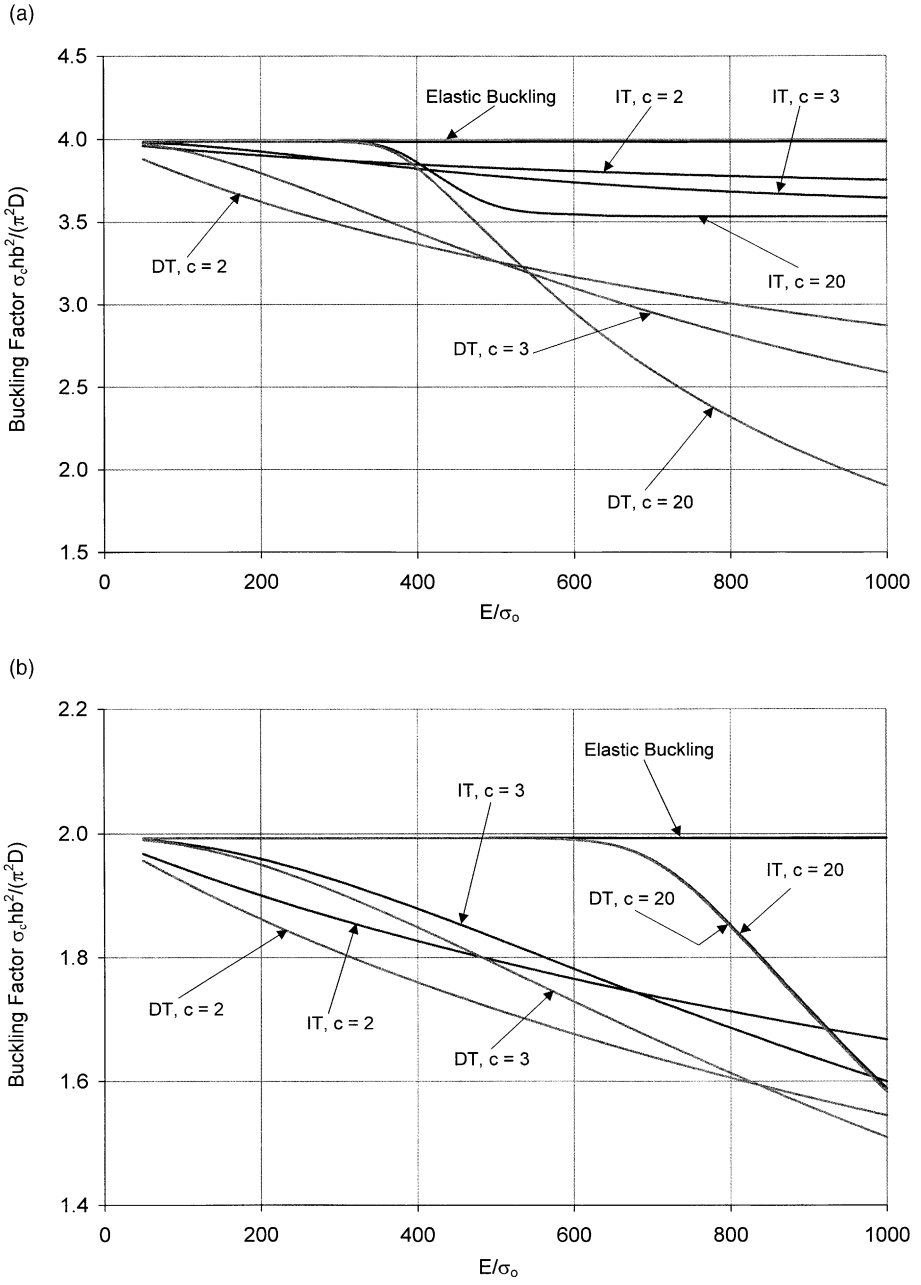

Fig. 4. Buckling stress factor $\sigma_c hb^2/(\pi^2 D)$ versus E/σ_0 for simply supported, square Mindlin plates subjected to (a) uniaxial load and (b) equibiaxial load ($a/b = 1,\ h/b = 0.025,\ \nu = 0.3,\ \kappa^2 = 5/6,\ k = 0.25$).

2.3. Buckling solutions for rectangular plates with two opposite sides simply supported

Next, we consider rectangular plates with two opposite edges simply supported (edges $y = 0$ and $y = b$), while the other edges (edge $x = 0$ and edge $x = a$) may take on any combination of free, simply supported

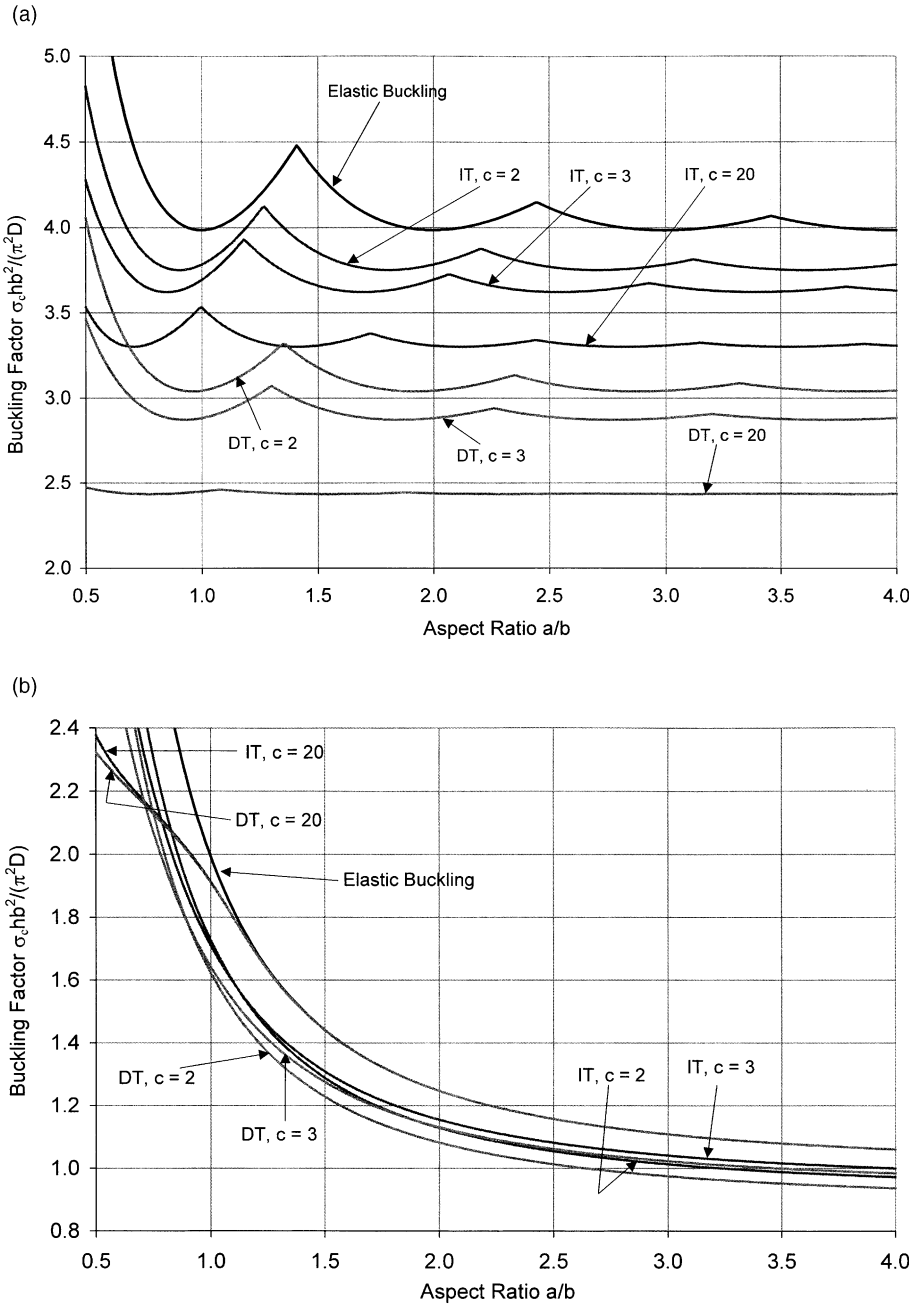

Fig. 5. Buckling stress factor $\sigma_c hb^2/(\pi^2 D)$ versus aspect ratio a/b for simply supported, rectangular Mindlin plates subjected to (a) uniaxial load and (b) equibiaxial load ($E/\sigma_0 = 750,\ h/b = 0.025,\ \nu = 0.3,\ \kappa^2 = 5/6,\ k = 0.25$).

and clamped edges. The boundary conditions for the two simply supported parallel edges ($y = 0$ and $y = b$) are

$$w(x,0) = M_{yy}(x,0) = \phi_x(x,0) = 0 \tag{18a}$$

$$w(x,b) = M_{yy}(x,b) = \phi_x(x,b) = 0 \tag{18b}$$

and the boundary conditions for the other two edges ($x = 0$ and $x = a$) are given by (Xiang et al., 1996)

$$M_{xx} = M_{yx} = 0, \qquad Q_x - \sigma_1 h \frac{\partial w}{\partial x} = 0 \quad \text{if the edge is free} \tag{19}$$

$$w = M_{xx} = \phi_y = 0 \quad \text{if the edge is simply supported} \tag{20}$$

$$w = \phi_x = \phi_y = 0 \quad \text{if the edge is clamped} \tag{21}$$

in which

$$Q_x = \kappa^2 Gh\left(\phi_x + \frac{\partial w}{\partial x}\right) \tag{22a}$$

$$M_{xx} = \frac{Eh^3}{12}\left(\alpha\frac{\partial \phi_x}{\partial x} + \beta\frac{\partial \phi_y}{\partial y}\right) \tag{22b}$$

$$M_{yy} = \frac{Eh^3}{12}\left(\beta\frac{\partial \phi_x}{\partial x} + \gamma\frac{\partial \phi_y}{\partial y}\right) \tag{22c}$$

$$M_{xy} = \frac{Gh^3}{12}\left(\frac{\partial \phi_x}{\partial y} + \frac{\partial \phi_y}{\partial x}\right) \tag{22d}$$

For such rectangular plates with two opposite sides simply supported, the Levy-type solution procedure may be used to solve the governing differential equations (Eqs. (11a)–(11c)) for buckling of plates. The velocity fields of the plate may be expressed as (Xiang et al., 1996)

$$\begin{Bmatrix} w(x,y) \\ \phi_x(x,y) \\ \phi_y(x,y) \end{Bmatrix} = \begin{Bmatrix} \eta_w(x)\sin\frac{m\pi y}{b} \\ \eta_x(x)\sin\frac{m\pi y}{b} \\ \eta_y(x)\cos\frac{m\pi y}{b} \end{Bmatrix} \tag{23}$$

in which $\eta_w(x)$, $\eta_x(x)$ and $\eta_y(x)$ are unknown functions to be determined, and $m = 1, 2, \ldots, \infty$ is the number of half waves of the buckling mode shape in the y-direction. Eq. (23) satisfies the simply supported boundary conditions on edges $y = 0$ and $y = b$.

Substituting Eq. (23) into Eqs. (11a)–(11c), the following differential equation system can be derived:

$$\boldsymbol{\psi}' = \mathbf{H}\boldsymbol{\psi} \tag{24}$$

where $\boldsymbol{\psi} = [\,\eta_w \quad \eta_w' \quad \eta_x \quad \eta_x' \quad \eta_y \quad \eta_y'\,]^{\mathrm{T}}$ and $\boldsymbol{\psi}'$ is the first derivative of $\boldsymbol{\psi}$ with respect to x, the prime ($'$) is the derivative with respect to x, and $\mathbf{H}$ is a (6×6) matrix with the following non-zero elements:

$$H_{12} = H_{34} = H_{56} = 1 \tag{25a}$$

$$H_{21} = \frac{(\kappa^2 Gh - \sigma_2 h)(m\pi/b)^2}{\kappa^2 Gh - \sigma_1 h} \tag{25b}$$

$$H_{24} = \frac{-\kappa^2 Gh}{\kappa^2 Gh - \sigma_1 h} \tag{25c}$$

$$H_{25} = \frac{\kappa^2 Gh(m\pi/b)}{\kappa^2 Gh - \sigma_1 h} \tag{25d}$$

$$H_{42} = \frac{-\kappa^2 Gh}{(\alpha Eh^3/12)} \tag{25e}$$

$$H_{43} = \frac{-\kappa^2 Gh + (Gh^3/12)(m\pi/b)^2}{(\alpha Eh^3/12)} \tag{25f}$$

$$H_{46} = \frac{[(\beta Eh^3/12) + (Gh^3/12)](m\pi/b)}{(\alpha Eh^3/12)} \tag{25g}$$

$$H_{61} = \frac{\kappa^2 Gh(m\pi/b)}{(Gh^3/12)} \tag{25h}$$

$$H_{64} = \frac{-[(\beta Eh^3/12) + (Gh^3/12)](m\pi/b)}{(Gh^3/12)} \tag{25i}$$

$$H_{65} = \frac{[\kappa^2 Gh + (\gamma Eh^3/12)(m\pi/b)^2]}{(Gh^3/12)} \tag{25j}$$

The solution of the differential equation system (Eq. (24)) can be obtained as

$$\mathbf{\Psi} = \mathbf{e}^{\mathbf{H}x}\mathbf{c} \tag{26}$$

where $\mathbf{c}$ is constant column vector that can be determined from the boundary conditions of the plate; and $\mathbf{e}^{\mathbf{H}x}$ is the general matrix solution. The detailed procedure in determining Eq. (26) may be found in an earlier paper by Xiang et al. (1996).

Applying the boundary conditions on the edges parallel to the y-axis, a homogeneous system of equations is obtained

$$\mathbf{Kc} = \mathbf{0} \tag{27}$$

The buckling stresses σ_1 and σ_2 are determined when the determinant of $\mathbf{K}$ is equal to zero. As the buckling stresses are imbedded in matrix $\mathbf{H}$, it cannot be obtained directly from Eq. (27). A numerical iteration procedure was used for the calculations (Xiang et al., 1996).

Tables 2–4 present the buckling stress factors of square plates under uniaxial and equibiaxial loads. In the calculations, $\kappa^2 = 5/6$ and $v = 0.3$ were taken. For brevity, we shall use the letters F for free edge, S for simply supported edge and C for clamped edge and a four-letter designation to represent the boundary conditions of the plate. So for example, a CSFS plate will have a clamped edge along $x = 0$, a simply supported edge along $y = 0$, a free edge along $x = a$ and a simply supported edge along $y = b$. It can be observed that for very thick plates ($h/b = 0.075$) and high values of c, the buckling load factors of the IT do not vary much with respect to the E/σ_0 ratios. In contrast, the corresponding buckling results from the DT decrease significantly with increasing E/σ_0 values for very thick plates. The buckling factors are much lower when compared to their thin plate counterparts due to the effect of transverse shear deformation.

Table 2
Buckling stress factors $\sigma_c hb^2/(\pi^2 D)$ for FSFS square plates under uniaxial load in the x-direction (Panel A), equibiaxial load (Panel B) ($\kappa^2 = 5/6$, $v = 0.3$, $k = 0.25$)

c	E/σ_0	$\sigma_c hb^2/(\pi^2 D)$					
		$h/b = 0.025$		$h/b = 0.050$		$h/b = 0.075$	
		IT	DT	IT	DT	IT	DT
Panel A							
Elastic	–	1.999	1.999	1.946	1.946	1.888	1.888
2	200	1.967	1.872	1.835	1.582	1.683	1.315
	300	1.952	1.819	1.794	1.473	1.624	1.188
	500	1.925	1.729	1.729	1.316	1.542	1.024
	750	1.895	1.637	1.669	1.183	1.476	0.8960
3	200	1.987	1.964	1.815	1.629	1.551	1.216
	300	1.974	1.925	1.722	1.447	1.433	1.015
	500	1.937	1.826	1.577	1.188	1.306	0.7831
	750	1.880	1.691	1.464	0.9834	1.236	0.6259
5	200	1.998	1.996	1.805	1.694	1.381	1.115
	300	1.994	1.988	1.624	1.424	1.240	0.8580
	500	1.965	1.926	1.392	1.060	1.133	0.5995
	750	1.875	1.765	1.279	0.8094	1.111	0.6013
10	200	1.999	1.999	1.828	1.786	1.226	1.0343
	300	1.999	1.999	1.520	1.413	1.113	0.8916
	500	1.994	1.992	1.242	0.9609	1.104	0.4835
	750	1.904	1.865	1.198	0.6882	1.104	0.3400
20	200	1.999	1.999	1.881	1.869	1.136	0.9993
	300	1.999	1.999	1.467	1.418	1.104	0.8187
	500	1.999	1.999	1.198	0.9164	1.104	0.4725
	750	1.958	1.949	1.196	0.6350	1.104	0.2978
Panel B							
Elastic	–	0.9280	0.9280	0.9207	0.9207	0.9106	0.9106
2	200	0.9147	0.8992	0.8735	0.8241	0.8195	0.7372
	300	0.9083	0.8860	0.8531	0.7882	0.7852	0.6856
	500	0.8961	0.8618	0.8173	0.7308	0.7306	0.6119
	750	0.8817	0.8348	0.7798	0.6766	0.6799	0.5493
3	200	0.9258	0.9241	0.8911	0.8693	0.8033	0.7468
	300	0.9232	0.9194	0.8605	0.8227	0.7304	0.6582
	500	0.9151	0.9052	0.7910	0.7302	0.6186	0.5346
	750	0.9004	0.8807	0.7116	0.6366	0.5291	0.4397
5	200	0.9279	0.9279	0.9118	0.9074	0.7964	0.7659
	300	0.9278	0.9277	0.8821	0.8670	0.6709	0.6314
	500	0.9265	0.9257	0.7701	0.7367	0.5072	0.4618
	750	0.9205	0.9170	0.6375	0.5966	0.4008	0.3495
10	200	0.9280	0.9280	0.9204	0.9204	0.8129	0.8021
	300	0.9280	0.9280	0.9125	0.9105	0.6298	0.6157
	500	0.9280	0.9280	0.7703	0.7582	0.4299	0.4114
	750	0.9278	0.9278	0.5843	0.5695	0.3189	0.2929
20	200	0.9280	0.9280	0.9207	0.9207	0.8461	0.8428
	300	0.9280	0.9280	0.9206	0.9207	0.6217	0.6174
	500	0.9280	0.9280	0.7914	0.7877	0.4000	0.3930
	750	0.9280	0.9280	0.5689	0.5641	0.2847	0.2717

Table 3
Buckling stress factors $\sigma_c hb^2/(\pi^2 D)$ for SSFS square plates under uniaxial load in the x-direction (Panel A), equibiaxial load (Panel B) ($\kappa^2 = 5/6$, $\nu = 0.3$, $k = 0.25$)

c	E/σ_0	$\sigma_c hb^2/(\pi^2 D)$					
		$h/b = 0.025$		$h/b = 0.050$		$h/b = 0.075$	
		IT	DT	IT	DT	IT	DT
Panel A							
Elastic	–	2.312	2.312	2.245	2.245	2.169	2.169
2	200	2.232	2.132	2.013	1.758	1.797	1.436
	300	2.199	2.061	1.943	1.624	1.714	1.288
	500	2.143	1.942	1.844	1.437	1.606	1.101
	750	2.086	1.824	1.759	1.283	1.523	0.9588
3	200	2.278	2.250	1.965	1.773	1.610	1.283
	300	2.242	2.185	1.822	1.549	1.466	1.060
	500	2.154	2.033	1.632	1.250	1.318	0.8113
	750	2.043	1.848	1.495	1.026	1.236	0.6456
5	200	2.307	2.305	1.926	1.809	1.402	1.143
	300	2.292	2.282	1.678	1.482	1.240	0.8736
	500	2.199	2.149	1.408	1.085	1.151	0.6074
	750	2.012	1.895	1.280	0.8234	1.134	0.4496
10	200	2.311	2.311	1.926	1.880	1.228	1.043
	300	2.311	2.311	1.544	1.439	1.135	0.7491
	500	2.280	2.272	1.248	0.9682	1.129	0.4850
	750	2.023	1.977	1.215	0.6915	1.129	0.3408
20	200	2.311	2.311	1.973	1.959	1.150	1.002
	300	2.311	2.311	1.479	1.430	1.129	0.6965
	500	2.310	2.310	1.215	0.9185	1.129	0.4350
	750	2.081	2.067	1.214	0.6358	1.129	0.2979
Panel B							
Elastic	–	1.046	1.046	1.032	1.032	1.015	1.015
2	200	1.034	1.010	0.9911	0.9162	0.9364	0.8112
	300	1.028	0.9942	0.9726	0.8738	0.9045	0.7521
	500	1.017	0.9649	0.9393	0.8070	0.8523	0.6686
	750	1.004	0.9325	0.9034	0.7446	0.8022	0.5985
3	200	1.044	1.041	1.004	0.9672	0.9112	0.8179
	300	1.041	1.034	0.9731	0.9102	0.8360	0.7164
	500	1.033	1.016	0.9016	0.8009	0.7195	0.5783
	750	1.018	0.9847	0.8180	0.6938	0.6276	0.4739
5	200	1.046	1.046	1.022	1.013	0.8859	0.8305
	300	1.045	1.045	0.9865	0.9569	0.7484	0.6772
	500	1.044	1.042	0.8577	0.7976	0.5791	0.4915
	750	1.036	1.029	0.7133	0.6394	0.4784	0.3708
10	200	1.046	1.046	1.032	1.032	0.8769	0.8551
	300	1.046	1.046	1.016	1.010	0.6749	0.6460
	500	1.046	1.046	0.8271	0.8036	0.4768	0.4291
	750	1.045	1.045	0.6280	0.5965	0.3928	0.3049
20	200	1.046	1.046	1.032	1.032	0.8919	0.8847
	300	1.046	1.046	1.031	1.032	0.6465	0.6362
	500	1.046	1.046	0.8266	0.8190	0.4306	0.4041
	750	1.046	1.046	0.5929	0.5808	0.3762	0.2791

Table 4
Buckling stress factors $\sigma_c hb^2/(\pi^2 D)$ for CSFS square plates under uniaxial load in the x-direction (Panel A), equibiaxial load (Panel B) ($\kappa^2 = 5/6$, $\nu = 0.3$, $k = 0.25$)

c	E/σ_0	$\sigma_c hb^2/(\pi^2 D)$					
		$h/b = 0.025$		$h/b = 0.050$		$h/b = 0.075$	
		IT	DT	IT	DT	IT	DT
Panel A							
Elastic	–	2.336	2.336	2.268	2.268	2.189	2.189
2	200	2.251	2.150	2.022	1.767	1.801	1.441
	300	2.217	2.077	1.950	1.631	1.716	1.292
	500	2.157	1.955	1.848	1.442	1.607	1.103
	750	2.097	1.835	1.761	1.287	1.523	0.9602
3	200	2.300	2.271	1.972	1.780	1.611	1.285
	300	2.262	2.204	1.825	1.553	1.466	1.061
	500	2.168	2.046	1.632	1.252	1.319	0.8117
	750	2.052	1.856	1.495	1.027	1.237	0.6458
5	200	2.332	2.329	1.931	1.815	1.402	1.144
	300	2.315	2.304	1.679	1.483	1.241	0.8737
	500	2.215	2.163	1.408	1.085	1.153	0.6074
	750	2.019	1.901	1.281	0.8235	1.136	0.4496
10	200	2.336	2.336	1.929	1.883	1.228	1.043
	300	2.336	2.335	1.544	1.439	1.137	0.7491
	500	2.300	2.292	1.250	0.9682	1.131	0.4850
	750	2.028	1.982	1.217	0.6915	1.131	0.3408
20	200	2.336	2.336	1.976	1.962	1.151	1.002
	300	2.336	2.336	1.479	1.431	1.131	0.6965
	500	2.335	2.335	1.216	0.9185	1.131	0.4351
	750	2.085	2.071	1.215	0.6358	1.131	0.2979
Panel B							
Elastic	–	1.130	1.130	1.112	1.112	1.090	1.090
2	200	1.119	1.089	1.075	0.9807	1.020	0.8622
	300	1.114	1.071	1.059	0.9335	0.9913	0.7976
	500	1.104	1.038	1.028	0.8597	0.9431	0.7070
	750	1.092	1.001	0.9953	0.7914	0.8956	0.6316
3	200	1.128	1.124	1.084	1.035	0.9907	0.8656
	300	1.125	1.116	1.055	0.9704	0.9171	0.7551
	500	1.118	1.094	0.9852	0.8488	0.7997	0.6070
	750	1.103	1.058	0.9016	0.7321	0.7059	0.4962
5	200	1.130	1.130	1.100	1.086	0.9530	0.8729
	300	1.130	1.129	1.062	1.018	0.8101	0.7073
	500	1.128	1.125	0.9253	0.8380	0.6381	0.5110
	750	1.119	1.108	0.7749	0.6678	0.5426	0.3847
10	200	1.130	1.130	1.111	1.111	0.9227	0.8886
	300	1.130	1.130	1.087	1.075	0.7118	0.6659
	500	1.130	1.130	0.8698	0.8331	0.5225	0.4406
	750	1.130	1.129	0.6652	0.6146	0.4713	0.3124
20	200	1.130	1.130	1.112	1.112	0.9207	0.9090
	300	1.130	1.130	1.109	1.112	0.6674	0.6489
	500	1.130	1.130	0.8514	0.8386	0.4771	0.4109
	750	1.130	1.130	0.6147	0.5920	0.4675	0.2832

In general, the DT gives consistently lower values of buckling stress factor when compared to the corresponding results obtained using the IT. The difference between the results of these two theories tends to increase with increasing thickness ratios, E/σ_0 values and the c values of the Ramberg–Osgood relation.

3. Axisymmetric buckling of circular plates

3.1. Basic equations

Consider a circular plate with radius a and uniform thickness h. The plate is subjected to uniform compressive radial stress of magnitude σ. According to the Mindlin plate theory, the admissible velocity field for axisymmetric deformation is given by

$$v_r = z\phi; \qquad v_\theta = 0; \qquad v_z = w \tag{28}$$

where ϕ is the rate of rotation and w the transverse velocity. For axisymmetric buckling, the non-zero strain rates associated with Eq. (28) are given by

$$\dot{\varepsilon}_{rr} = z\frac{\mathrm{d}\phi}{\mathrm{d}r}; \qquad \dot{\varepsilon}_{\theta\theta} = z\frac{\phi}{r}; \qquad \dot{\gamma}_{rz} = \phi + \frac{\mathrm{d}w}{\mathrm{d}r} \tag{29}$$

The constitutive relations are given by

$$\dot{\sigma}_{rr} = E(\alpha\dot{\varepsilon}_{rr} + \beta\dot{\varepsilon}_{\theta\theta}); \qquad \dot{\sigma}_{\theta\theta} = E(\beta\dot{\varepsilon}_{rr} + \alpha\dot{\varepsilon}_{\theta\theta}); \qquad \dot{\tau}_{rz} = \kappa^2 G\dot{\gamma}_{rz} \tag{30}$$

where E is the Young's modulus, κ^2 the shear correction factor and the parameters α, β, γ are given by

$$\alpha = \frac{1}{\rho}\left[4 - 3\left(1 - \frac{T}{S}\right)\right] \tag{31a}$$

$$\beta = \frac{1}{\rho}\left[2 - 2(1-2\nu)\frac{T}{E} - 3\left(1 - \frac{T}{S}\right)\right] \tag{31b}$$

$$\rho = 3\frac{E}{S} + (1-2\nu)\left[2 - (1-2\nu)\frac{T}{E} - 3\left(1 - \frac{T}{S}\right)\right] \tag{31c}$$

and the ratios of the elastic modulus E to the shear modulus G, the tangent modulus T, secant modulus S at the onset of buckling are given in Eqs. (5)–(7). Note that the preceding expressions of α, β, ρ describe the constitutive equations based on the rate form of Hencky's stress–strain relation. By setting $S = E$, these expressions reduce to those corresponding to the Prandtl–Reuss constitutive relation.

To obtain the condition for bifurcation of the plate in the elastic/plastic range, consider the uniqueness criterion which takes the form of

$$\int \left\{ (\dot{\sigma}_{rr}\dot{\varepsilon}_{rr} + \dot{\sigma}_{\theta\theta}\dot{\varepsilon}_{\theta\theta} + \dot{\tau}_{rz}\dot{\gamma}_{rz}) - \sigma\left(\frac{\mathrm{d}w}{\mathrm{d}r}\right)^2 \right\} \mathrm{d}V > 0 \tag{32}$$

Using Eqs. (29) and (30) and integrating through the thickness of the plate, the condition for uniqueness is reduced to

$$\int\int \left\{ \frac{\alpha E h^3}{12}\left(\frac{\mathrm{d}\phi}{\mathrm{d}r}\right)^2 + \frac{\alpha E h^3}{12}\left(\frac{\phi}{r}\right)^2 + \frac{\beta E h^3}{6}\left(\frac{\phi}{r}\right)\left(\frac{\mathrm{d}\phi}{\mathrm{d}r}\right) + \kappa^2 G h\left(\phi + \frac{\mathrm{d}w}{\mathrm{d}r}\right)^2 - \sigma h\left(\frac{\mathrm{d}w}{\mathrm{d}r}\right)^2 \right\} r\,\mathrm{d}r > 0 \tag{33}$$

The Euler–Lagrange differential equations associated with the minimization with respect to arbitrary variations of w, and ϕ are easily shown to be

$$\kappa^2 Gh\left(\phi + \frac{\mathrm{d}w}{\mathrm{d}r}\right) = \sigma h \frac{\mathrm{d}w}{\mathrm{d}r} \Rightarrow \frac{\mathrm{d}w}{\mathrm{d}r} = -\frac{\phi}{1-(\sigma/\kappa^2 G)} \tag{34a}$$

and

$$\frac{\alpha Eh^3}{12} r \frac{\mathrm{d}^2\phi}{\mathrm{d}r^2} + \frac{\alpha Eh^3}{12}\frac{\mathrm{d}\phi}{\mathrm{d}r} - \frac{\alpha Eh^3}{12}\frac{\phi}{r} - r\kappa^2 Gh\left(\phi + \frac{\mathrm{d}w}{\mathrm{d}r}\right) = 0 \tag{34b}$$

When the bifurcation occurs in the elastic range (i.e. $T = S = E$), we have α given by Eq. (12a), respectively, and Eqs. (34a) and (34b) reduce to the well-known governing equation for elastic buckling of circular Mindlin plates (Hong et al., 1993).

3.2. Axisymmetric buckling solutions of circular plates

Eliminating the derivative of w in Eq. (34b) by using Eq. (34a), one obtains

$$r^2 \frac{\mathrm{d}^2\phi}{\mathrm{d}r^2} + r\frac{\mathrm{d}\phi}{\mathrm{d}r} + (\xi^2 - 1)\phi = 0 \tag{35}$$

where

$$\xi = r\sqrt{\left(\frac{\sigma h}{1-(\sigma/\kappa^2 G)}\right)\frac{12}{\alpha Eh^3}} \tag{36}$$

Eq. (35) is a Bessel's differential equation with the general solution

$$\phi = AJ_1(\xi) + BY_1(\xi) \tag{37}$$

where A, B are constants, $J_1(\xi)$, $Y_1(\xi)$ are first order Bessel functions of the first kind and second kind, respectively. Since from axisymmetric condition $\phi = 0$ at the plate centre (i.e. at $r = \xi = 0$), the constant B must vanish in Eq. (37). Thus Eq. (37) reduces to

$$\phi = AJ_1(\xi) \tag{38}$$

The critical stress would evidently depend on the support condition at the edge at $r = a$.

3.3. Clamped circular plate

For a clamped circular plate, the rotation at the edge must vanish at the edge, i.e. $\phi = 0$ at $r = a$. Thus in view of this boundary condition and Eq. (38), the bifurcation criterion is given by,

$$J_1(\lambda) = 0 \tag{39}$$

where, in view of Eqs. (31a) and (36),

$$\lambda = a\sqrt{\left(\frac{\sigma h}{1-(\sigma/\kappa^2 G)}\right)\frac{12}{\alpha Eh^3}} \tag{40}$$

Since λ involves σ/E for any given stress–strain curve, the solution must be found by an iterative method, such as the false position method.

3.4. Simply supported circular plate

For a simply supported circular plate, the bending moment in the radial direction must vanish at the edge, i.e. $d\phi/d\xi + (\beta\phi)/(\alpha\xi) = 0$ at $r = a$. Thus, in view of Eqs. (31a) and (31b), using Eq. (38) and noting the fact that $J_1'(\xi) = J_0(\xi) - (1/\xi)J_1(\xi)$, we obtain the bifurcation criterion as,

$$\frac{\lambda J_0(\lambda)}{J_1(\lambda)} = 1 - \frac{\beta}{\alpha} \tag{41}$$

Since the left hand side of this equation depends on the value of σ/E, the critical stress has to be computed iteratively.

Tables 5 and 6 present the buckling stress factors for simply supported and clamped circular plates, respectively, for various values of c and thickness-to-radius ratios h/a. In the calculations, $\kappa^2 = 5/6$ and $v = 0.3$ were taken. The elastic buckling stress factors, obtained by setting $T = S = E$, are also given for comparison purposes and these elastic results check out with those obtained by Kanaka Raju and Venkateswara Rao (1983) and Hong et al. (1993).

Based on the buckling stress factors in these tables, we observe that

(a) For simply supported plates, the buckling stress factors decrease with increasing plate thickness h/a, but may increase or decrease depending on the values of E/σ_0 and c. Both theories of plasticity give more or less similar buckling stress factors with the IT furnishing slightly higher results. Fig. 6 shows the

Table 5
Buckling stress factors $\sigma_c ha^2/(\pi^2 D)$ for simply supported circular plates ($\kappa^2 = 5/6$, $v = 0.3$, $k = 0.25$)

c	E/σ_0	$\sigma_c ha^2/(\pi^2 D)$					
		$h/a = 0.025$		$h/a = 0.050$		$h/a = 0.075$	
		IT	DT	IT	DT	IT	DT
Elastic	–	0.4250	0.4250	0.4241	0.4241	0.4225	0.4225
2	200	0.4185	0.4181	0.4002	0.3988	0.3756	0.3728
	300	0.4153	0.4147	0.3902	0.3881	0.3586	0.3549
	500	0.4094	0.4084	0.3726	0.3697	0.3317	0.3270
	750	0.4024	0.4010	0.3545	0.3507	0.3067	0.3010
3	200	0.4245	0.4245	0.4167	0.4164	0.3919	0.3907
	300	0.4239	0.4239	0.4086	0.4079	0.3665	0.3644
	500	0.4220	0.4219	0.3875	0.3861	0.3198	0.3168
	750	0.4185	0.4182	0.3589	0.3568	0.2757	0.2720
5	200	0.4250	0.4250	0.4236	0.4236	0.4121	0.4118
	300	0.4250	0.4250	0.4217	0.4217	0.3850	0.3843
	500	0.4249	0.4249	0.4087	0.4084	0.3160	0.3146
	750	0.4246	0.4246	0.3744	0.3735	0.2518	0.2500
10	200	0.4250	0.4250	0.4241	0.4241	0.4221	0.4221
	300	0.4250	0.4250	0.4240	0.4240	0.4121	0.4120
	500	0.4250	0.4250	0.4231	0.4231	0.3258	0.3253
	750	0.4250	0.4250	0.4028	0.4026	0.2413	0.2407
20	200	0.4250	0.4250	0.4241	0.4241	0.4225	0.4225
	300	0.4250	0.4250	0.4241	0.4241	0.4222	0.4221
	500	0.4250	0.4250	0.4241	0.4241	0.3425	0.3424
	750	0.4250	0.4250	0.4217	0.4217	0.2429	0.2427

Table 6
Buckling stress factors $\sigma_c ha^2/(\pi^2 D)$ for clamped circular plates ($\kappa^2 = 5/6$, $v = 0.3$, $k = 0.25$)

c	E/σ_0	$\sigma_c ha^2/(\pi^2 D)$					
		$h/a = 0.025$		$h/a = 0.050$		$h/a = 0.075$	
		IT	DT	IT	DT	IT	DT
Elastic	–	1.484	1.484	1.472	1.472	1.453	1.453
2	200	1.431	1.409	1.307	1.241	1.176	1.069
	300	1.408	1.377	1.252	1.166	1.105	0.9742
	500	1.367	1.320	1.168	1.055	1.009	0.8483
	750	1.323	1.260	1.094	0.9573	0.9326	0.7481
3	200	1.470	1.466	1.320	1.282	1.086	1.001
	300	1.453	1.445	1.218	1.158	0.9573	0.8458
	500	1.409	1.388	1.060	0.9677	0.8072	0.6601
	750	1.342	1.306	0.9296	0.8107	0.7092	0.5311
5	200	1.483	1.483	1.364	1.348	0.9997	0.9467
	300	1.480	1.480	1.203	1.171	0.8168	0.7388
	500	1.460	1.456	0.9534	0.8941	0.6443	0.5223
	750	1.390	1.377	0.7779	0.6918	0.5638	0.3901
10	200	1.484	1.484	1.438	1.436	0.9425	0.9206
	300	1.484	1.484	1.229	1.218	0.7133	0.6721
	500	1.483	1.483	0.8782	0.8521	0.5442	0.4415
	750	1.461	1.460	0.6678	0.6182	0.5176	0.3127
20	200	1.484	1.484	1.471	1.471	0.9316	0.9243
	300	1.484	1.484	1.283	1.279	0.6689	0.6500
	500	1.484	1.484	0.8550	0.8456	0.5178	0.4112
	750	1.483	1.483	0.6182	0.5925	0.5164	0.2836

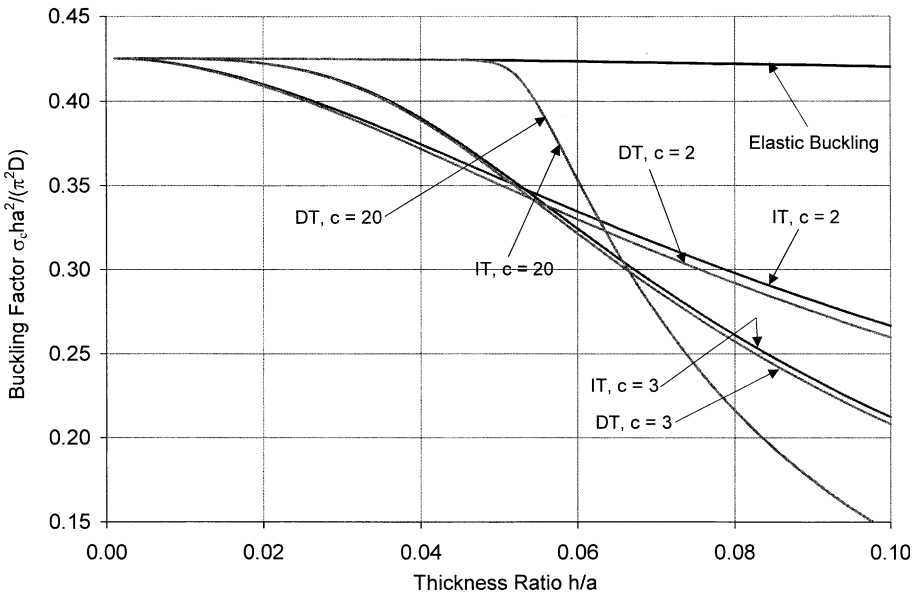

Fig. 6. Buckling stress factor $\sigma_c ha^2/(\pi^2 D)$ versus thickness ratio h/a for simply supported circular Mindlin plates subjected to uniform radial load ($E/\sigma_0 = 750,\ v = 0.3,\ \kappa^2 = 5/6,\ k = 0.25$).

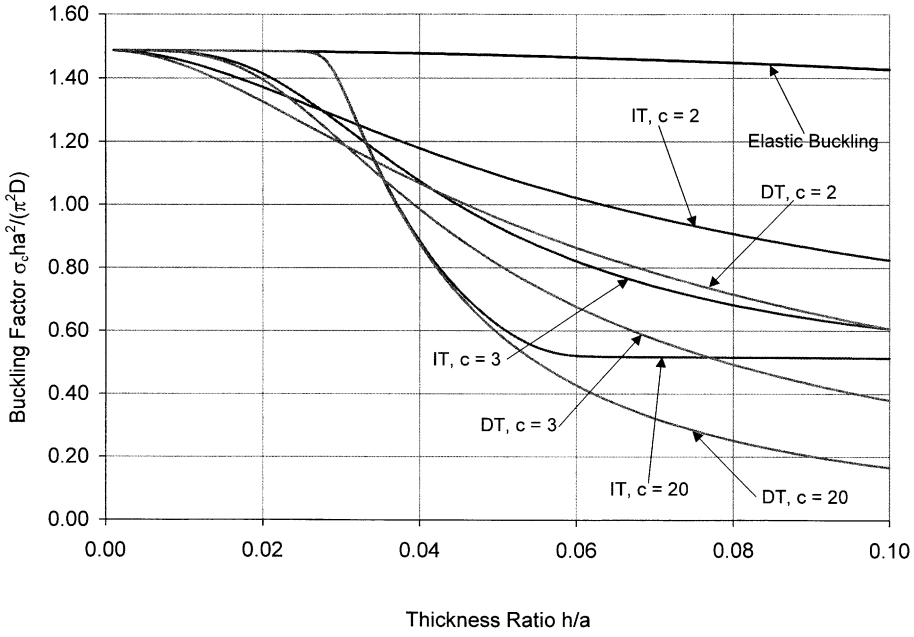

Fig. 7. Buckling stress factor $\sigma_c ha^2/(\pi^2 D)$ versus thickness ratio h/a for clamped circular Mindlin plates subjected to uniform radial load ($E/\sigma_0 = 750,\ \nu = 0.3,\ \kappa^2 = 5/6,\ k = 0.25$).

difference between the buckling results of the two theories for $E/\sigma_0 = 750$ for simply supported circular plates.

(b) For clamped plates, the buckling stress factors decrease with increasing plate thickness h/a, but may increase or decrease depending on the values of E/σ_0 and c. In contrast to the simply supported plate case, we see that buckling stress factors of clamped plates differ significantly using the IT and the DT. Fig. 7 shows the difference between the buckling results of the two theories for $E/\sigma_0 = 750$ for clamped circular plates.

4. Concluding remarks

The elastic/plastic buckling equations for thick plates are presented. The Mindlin plate theory was adopted to admit the effect of transverse shear deformation which becomes significant in thick plates. To capture the more practical elastic/plastic behaviour, two competing plasticity theories are considered; i.e. the incremental theory of plasticity (IT) with the Prandtl–Reuss constitutive equations and the deformation theory of plasticity (DT) with the Hencky constitutive equations. The stability criteria are derived for uniaxially loaded and equibiaxially loaded rectangular plates and uniform radially loaded circular plates. Extensive closed form buckling stresses were generated for the square and circular plates with the Ramberg–Osgood elastoplastic characteristic.

Generally, plastic buckling stress factors are much reduced from its elastic counterparts, especially when the plate is thick, E/σ_0 and Ramberg–Osgood constant c have large values. The buckling stress factors obtained using the DT are consistently lower than the corresponding factors of the IT. The divergence of these two results increases with increasing plate thickness, E/σ_0 and c values. This marked difference in

buckling stress factors observed for thick plates could be exploited when designing experimental tests on plates to establish which of the two considered theories of plasticity give better buckling results for thick plates.

Acknowledgements

The first author would like to thank his colleague, W.A.M. Alwis, for very useful discussion in the course of this work.

Appendix A. Derivation of constitutive relations based on the rate form of Hencky's deformation theory

It is assumed that the relationship between the stress rate and the rate of deformation at the point of bifurcation is that corresponding to the incremental form of the DT suggested by Hencky. Since the strain rate vector in that case is not along the normal to the Mises yield surface in the stress space, the yield surface must be supposed to have locally changed in shape so that the normality rule still holds. The possibility of the formation of a corner on the yield surface may also be included. The parameter $\bar{\sigma}$ in this modified theory is simply a measure of the length of the current deviatoric stress vector, rather than that of the radius of an isotropically expanding Mises cylinder. The incremental form of the Hencky equation $\varepsilon_{ij}^{\mathrm{p}} = (3\bar{\varepsilon}^{\mathrm{p}}/2\bar{\sigma})s_{ij}$ is easily found as

$$\mathrm{d}\varepsilon_{ij}^{\mathrm{p}} = \frac{3\,\mathrm{d}\bar{\sigma}}{2\bar{\sigma}}\left(\frac{\mathrm{d}\bar{\varepsilon}^{\mathrm{p}}}{\mathrm{d}\bar{\sigma}} - \frac{\bar{\varepsilon}^{\mathrm{p}}}{\bar{\sigma}}\right)s_{ij} + \frac{3\bar{\varepsilon}^{\mathrm{p}}}{2\bar{\sigma}}\mathrm{d}s_{ij} \tag{A.1}$$

where s_{ij} is the deviatoric stress vector, and $\mathrm{d}s_{ij}$ is its time increment, which must be considered in the Jaumann sense, so that it vanishes in the event of an instantaneous rigid body rotation. The elastic strain increment, given by the generalized Hooke's law, is

$$\mathrm{d}\varepsilon_{ij}^{\mathrm{e}} = \left(\frac{1+v}{E}\right)\mathrm{d}s_{ij} + \left(\frac{1-2v}{3E}\right)\delta_{ij}\,\mathrm{d}\sigma_{kk} \tag{A.2}$$

where δ_{ij} is the Kronecker delta.

Combining Eqs. (A.1) and (A.2), the rate form of the complete stress–strain relation is obtained as

$$E\dot{\varepsilon}_{ij} = \left(\frac{3E}{2S} - \frac{1-2v}{2}\right)\dot{s}_{ij} + \left(\frac{1-2v}{3}\right)\dot{\sigma}_{kk}\delta_{ij} + \frac{3\dot{\bar{\sigma}}}{2\bar{\sigma}}\left(\frac{E}{T} - \frac{E}{S}\right)s_{ij} \tag{A.3}$$

during the continued loading of a plastically stressed element. Although the preceding equation looks much more complicated than the Prandtl–Reuss equation, the final results are not so for a biaxial state of stress. In the above, T is the tangent modulus equal to $\mathrm{d}\bar{\sigma}/\mathrm{d}\bar{\varepsilon}$, and S is the secant modulus equal to $\bar{\sigma}/\bar{\varepsilon}$, where $\bar{\varepsilon}$ is the total effective strain.

Let $-\sigma_1$ and $-\sigma_2$ denote the non-zero principal stresses whose directions coincide with the x and y axes, respectively, at the point of bifurcation. Since the effective stress $\bar{\sigma}$ is given by

$$\bar{\sigma}^2 = \sigma_x^2 - \sigma_x\sigma_y + \sigma_y^2 + 3\tau_{xy}^2 \tag{A.4}$$

a straightforward differentiation gives

$$\frac{\mathrm{d}\bar{\sigma}}{\bar{\sigma}} = -\frac{(2\sigma_1 - \sigma_2)\mathrm{d}\sigma_x + (2\sigma_2 - \sigma_1)\mathrm{d}\sigma_y}{2\bar{\sigma}^2} \tag{A.5}$$

on setting $\sigma_x = -\sigma_1$, $\tau_{xy} = 0$, $\sigma_y = -\sigma_2$ at bifurcation. The constitutive Eq. (A.3) therefore furnishes

$$E\dot{\varepsilon}_x = \frac{1}{2}\left(\frac{E}{S} - \frac{1-2v}{3}\right)(2\dot{\sigma}_x - \dot{\sigma}_y) + \frac{1-2v}{3}(\dot{\sigma}_x + \dot{\sigma}_y) + \frac{2\sigma_1 - \sigma_2}{4\bar{\sigma}^2}[(2\sigma_1 - \sigma_2)\dot{\sigma}_x + (2\sigma_2 - \sigma_1)\dot{\sigma}_y] \tag{A.6}$$

$$E\dot{\varepsilon}_y = \frac{1}{2}\left(\frac{E}{S} - \frac{1-2v}{3}\right)(2\dot{\sigma}_y - \dot{\sigma}_x) + \frac{1-2v}{3}(\dot{\sigma}_x + \dot{\sigma}_y) + \frac{2\sigma_2 - \sigma_1}{4\bar{\sigma}^2}[(2\sigma_1 - \sigma_2)\dot{\sigma}_x + (2\sigma_2 - \sigma_1)\dot{\sigma}_y] \tag{A.7}$$

$$E\dot{\varepsilon}_{xy} = \frac{1}{2}\left(\frac{3E}{S} - (1-2v)\right)\dot{\tau}_{xy} \tag{A.8}$$

After some algebraic manipulations, the first two results are reduced to

$$T\dot{\varepsilon}_x = \left[1 - \frac{3}{4}\left(1 - \frac{T}{S}\right)\frac{\sigma_2^2}{\bar{\sigma}^2}\right]\dot{\sigma}_x - \left[\eta - \frac{3}{4}\left(1 - \frac{T}{S}\right)\frac{\sigma_1\sigma_2}{\bar{\sigma}^2}\right]\dot{\sigma}_y \tag{A.9}$$

$$T\dot{\varepsilon}_y = \left[1 - \frac{3}{4}\left(1 - \frac{T}{S}\right)\frac{\sigma_1^2}{\bar{\sigma}^2}\right]\dot{\sigma}_y - \left[\eta - \frac{3}{4}\left(1 - \frac{T}{S}\right)\frac{\sigma_1\sigma_2}{\bar{\sigma}^2}\right]\dot{\sigma}_x \tag{A.10}$$

where η is the contraction ratio at the current state of stress. On using the expression $\sigma_1^2 - \sigma_1\sigma_2 + \sigma_2^2 = \bar{\sigma}^2$, the above relations can be inverted to give the constitutive relations in the form

$$\dot{\sigma}_x = E(\alpha\dot{\varepsilon}_x + \beta\dot{\varepsilon}_y), \qquad \dot{\sigma}_y = E(\beta\dot{\varepsilon}_x + \gamma\dot{\varepsilon}_y), \qquad \dot{\tau}_{xy} = \frac{2E\dot{\varepsilon}_{xy}}{[2v + ((3E/S) - 1)]} \tag{A.11}$$

where

$$\begin{aligned}
\alpha &= \frac{1}{\rho}\left[4 - 3\left(1 - \frac{T}{S}\right)\frac{\sigma_1^2}{\bar{\sigma}^2}\right] \\
\beta &= \frac{1}{\rho}\left[2 - 2(1-2v)\frac{T}{E} - 3\left(1 - \frac{T}{S}\right)\frac{\sigma_1\sigma_2}{\bar{\sigma}^2}\right] \\
\gamma &= \frac{1}{\rho}\left[4 - 3\left(1 - \frac{T}{S}\right)\frac{\sigma_2^2}{\bar{\sigma}^2}\right] \\
\rho &= \frac{3E}{S} + (1-2v)\left[2 - (1-2v)\frac{T}{E} - 3\left(1 - \frac{T}{S}\right)\frac{\sigma_1\sigma_2}{\bar{\sigma}^2}\right]
\end{aligned} \tag{A.12}$$

Appendix B. Derivation of constitutive relations based on the Prandtl–Reuss material

For a Prandtl–Reuss material, the plastic strain rate vector, in a nine dimensional space, is directed along the deviatoric stress vector. Stated mathematically, the flow rule is

$$\dot{\varepsilon}_{ij}^{\mathrm{p}} = \frac{3\dot{\bar{\varepsilon}}^{\mathrm{p}}}{2\bar{\sigma}}s_{ij} = \frac{3\dot{\bar{\sigma}}}{2H\bar{\sigma}}s_{ij} = \frac{3\dot{\bar{\sigma}}}{2\bar{\sigma}}\left(\frac{1}{T} - \frac{1}{E}\right)s_{ij} \tag{B.1}$$

since

$$\frac{1}{H} = \frac{\mathrm{d}\bar{\varepsilon}^{\mathrm{p}}}{\mathrm{d}\bar{\sigma}} = \frac{\mathrm{d}\bar{\varepsilon} - \mathrm{d}\bar{\varepsilon}^{\mathrm{e}}}{\mathrm{d}\bar{\sigma}} = \frac{\mathrm{d}\bar{\varepsilon}}{\mathrm{d}\bar{\sigma}} - \frac{1}{E} = \frac{1}{T} - \frac{1}{E} \tag{B.2}$$

The complete Prandtl–Reuss equation relating the stress rate to the strain rate is given by

$$E\dot{\varepsilon}_{ij} = (1+v)\dot{s}_{ij} + \left(\frac{1-2v}{3}\right)\dot{\sigma}_{kk}\delta_{ij} + \frac{3\dot{\bar{\sigma}}}{2\bar{\sigma}}\left(\frac{E}{T}-1\right)s_{ij} \tag{B.3}$$

This equation may be compared with Eq. (A.3), which evidently reduces Eq. (B.3) on setting $S = E$ in the first and last terms on the right hand side. The method of derivation of the biaxial constitutive relations is similar to that employed before.

It should be noted that the use of Eq. (A.3) for the analysis of the bifurcation problem, which is essentially incremental in nature, along with the rate form of the field equations, is equivalent to the adoption of a physically acceptable IT of plasticity. The DT, on the other hand, is based on stress and displacement fields (not their rates of change), together with the integrated form of Eq. (A.3) as proposed by Hencky. The results obtained from the two approaches are bound to differ from one another.

References

Bartdorf, S.B., 1949. Theories of plastic buckling. Journal of the Aeronautical Sciences 16, 405–408.

Bazant, Z.P., Cedolin, L., 1991. Stability of Structures. Oxford University Press, New York.

Bijlaard, P.P., 1949. Theory and tests on the plastic stability of plates and shells. Journal of the Aeronautical Sciences 9, 529–541.

Bleich, F., 1952. Buckling Strength of Metal Structures. McGraw-Hill, New York.

Brunelle, E.J., 1971. Buckling of transversely isotropic Mindlin plates. AIAA Journal 9 (6), 1018–1022.

Chakrabarty, J., 2000. Applied Plasticity. Springer, New York.

Chen, L.W., Doong, J.L., 1984. Postbuckling behaviour of a thick circular plate. AIAA Journal 22, 564–566.

Dumir, P.C., 1985. Axisymmetric postbuckling of orthotropic tapered thick annular plates. Transactions of the ASME, Journal of Applied Mechanics 52, 725–727.

Durban, D., Zuckerman, Z., 1999. Elastoplastic buckling of rectangular plates in biaxial compression/tension. International Journal of Mechanical Science 41, 751–765.

El-Ghazaly, H.A., Sherbourne, A.N., 1986. Deformation theory for elastic–plastic buckling analysis of plates under non-proportional planar loading. Computers and Structures 22 (2), 131–149.

Handelman, G.H., Prager, W., 1948. Plastic buckling of rectangular plates under edge thrusts. Tech. Note, NACA-1530.

Herrmann, G., Armenakas, A.E., 1960. Vibrations and stability of plates under initial stress. Proceedings of the ASCE, Journal of Engineering Mechanics Division 86, 65–94.

Hong, G.M., Wang, C.M., Tan, T.J., 1993. Analytical buckling solutions for circular Mindlin plates: inclusion of inplane prebuckling deformation. Archive of Applied Mechanics 63, 534–542.

Illyushin, A.A., 1947. The elastic plastic stability of plates. Tech. Note, NACA-1188.

Inoue, T., Kato, B., 1993. Analysis of plastic buckling of steel plates. International Journal of Solids and Structures 30 (6), 835–856.

Kanaka Raju, K., Venkateswara Rao, G., 1983. Postbuckling analysis of moderately thick elastic circular plates. Transactions of the ASME, Journal of Applied Mechanics 50, 468–470.

Kaufmann, W., 1936. Uber unelastisches Knicken rechtiger Platten. Ingenieur Archiv. 7 (6), 156.

Kollbrunner, C.F., 1946. Das Ausbeulun der auf einseitigen, gleichmassig verteilten Druck beanspruchten Platten im elastichen und plastichen Bereich. Mitteilungen 17, Institut fur Baustatic, Eidgenossische Technische Hoschule, Zurich.

Mindlin, R.D., 1951. Influence of rotatory inertia and shear on flexural motions of isotropic, elastic plates. Transactions of the ASME, Journal of Applied Mechanics 18, 31–38.

Ore, E., Durban, D., 1989. Elastoplastic buckling of annular plates in pure shear. Transactions of the ASME, Journal of Applied Mechanics 56, 644–651.

Pearson, C.E., 1950. Bifurcation criteria and plastic buckling of plates and columns. Journal of the Aeronautical Sciences 7, 417–424.

Shrivastava, S.C., 1979. Inelastic buckling of plates including shear effects. International Journal of Solids and Structures 15, 567–575.

Stowell, E.Z., 1948. A unified theory of plastic buckling of columns and plates. Tech. Note, NACA-1556.

Timoshenko, S.P., Gere, J.M., 1961. Theory of Elastic Stability. McGraw-Hill, New York.

Tugcu, P., 1991. Plate buckling in the plastic range. International Journal of Mechanical Science 33 (1), 1–11.

Xiang, Y., Liew, K.M., Kitipornchai, S., 1996. Exact buckling solutions for composite laminates: Proper free edge conditions under in-plane loadings. Acta Mechanica 117 (3–4), 115–128.

Wang, C.M., 1995. Allowance for prebuckling deformations in buckling load relationship between Mindlin and Kirchhoff simply supported plates of general polygonal shape. Engineering Structures 17 (6), 413–418.

Wang, C.M., Tan, T.J., Hong, G.M., Alwis, W.A.M., 1996. Buckling of tapered circular plates: allowances for effects of shear and radial deformation. Mechanics of Structures and Machines 24 (2), 135–153.

Wang, C.M., Xiang, Y., Kitipornchai, S., 1993. Axisymmetric buckling of circular Mindlin plates with ring supports. Journal of Structural Engineering, ASCE 119 (3), 782–793.